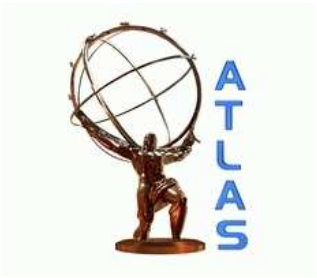

ATLAS NOTE

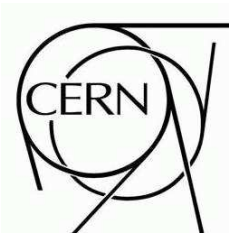

April 28, 2009

Study of Signal and Background Conditions in $t\bar{t}H, H \rightarrow WW^{(*)}$ and $WH, H \rightarrow WW^{(*)}$

The ATLAS Collaboration[1)]

This note is part of CERN-OPEN-2008-020. This version of the note should not be cited: all citations should be to CERN-OPEN-2008-020.

Abstract

In this note we present Monte Carlo studies of the associated Standard Model Higgs boson production in the $t\bar{t}H$ and WH channels with the decay $H \rightarrow WW^{(*)}$. These channels are intended to provide information on the Higgs boson's couplings. We study the two- and three lepton final states in $t\bar{t}H$ and three lepton final states in WH, based on the full ATLAS detector simulation.

[1)]This note prepared by: Y. Bai, J. Elmsheuser, S. Jin, F. Lu, I. Ludwig, E. Monnier, B. Ruckert, L.Y. Shan, C. Weiser, H. Zhang.

ATL-PHYS-PUB-2009-058
10 May 2009

1 Introduction

The discovery and subsequent study of the Higgs boson is one of the main aims of the Large Hadron Collider (LHC) at CERN. The possible mass range of the Standard Model Higgs boson is bounded by the lower limit set at LEP of 114 GeV and reaches to about 1000 GeV [1]. The ATLAS experiment will use all possible channels to extract information on it, because comparing the rates in the different channels will allow information on the couplings to be extracted.

The sensitivity of ATLAS to a Higgs boson produced in gluon fusion or via vector boson fusion and decaying to W quark pairs has been discussed elsewhere in this volume [2]. This note contains the results of studies of the Higgs boson in the same decay mode but produced in association with either top quarks, ($t\bar{t}H, H \to WW^{(*)}$), or a W boson ($WH, H \to WW^{(*)}$). The cross-sections for these processes are significantly lower than for inclusive Higgs production, and the additional activity makes them more complex to reconstruct, but the presence of extra signatures gives more possibilities for the reduction of the background.

This note explores techniques to exploit these signatures, and the signal and background conditions are studied in both channels. A full simulation of the ATLAS experiment is employed to estimate these, which represents an improvement over the fast simulation used in previous studies of $t\bar{t}H$ [3] and WH [4, 5]. The marginal production rates and numerous background sources, many with large cross-sections, make this analysis difficult, and both the background and signal need to be established in some detail. Nevertheless, if the background can be well estimated, then for integrated luminosities of several tens of fb^{-1} measurements should be possible.

The backgrounds considered in detail here arise from the inclusive $t\bar{t}$ process, from $t\bar{t}$ produced in association with gauge bosons, and from gauge bosons produced inclusively or in pairs. Unfortunately, it has not been possible to model all the relevant backgrounds with a complete simulation at the statistical level required; this is true for example of inclusive QCD multijet events. Section 2 describes the considered signal and background processes. Sections 3 and 4 give the details of $t\bar{t}H$ and WH analysis accordingly. Section 5 discusses the results, including the signal-to-background ratio that can be achieved in these two channels.

2 Signal and background Monte Carlo samples

Signal and background were produced with various generators, through a realistic ATLAS detector simulation based on the GEANT 4 package [6].

2.1 Signal generation

Events with a Higgs boson decaying to a W pair produced in association with a $t\bar{t}$ pair or with a W boson can be searched for at hadron colliders by requiring the presence of lepton pairs ($\ell = e, \mu$).

In particular, for the two-lepton final states, like-sign leptons are selected; this allows a strong reduction of the large background produced by the Z or $t\bar{t}$ leptonic decays. In order to improve the efficiency of the Monte Carlo data sample production, generated events were filtered before their processing through the ATLAS detector simulation.

For the WH channel, only events with three leptons in the final state were selected. These leptons had to pass loose η and p_T cuts.

Samples of $t\bar{t}H$ with at least two leptons were generated and filtered for different Higgs boson masses between 120 and 200 GeV using the PYTHIA 6.4 generator [7]. Results obtained with these samples were normalized to the Next-to-Leading Order (NLO) cross-sections and branching ratios reported in

Ref. [1]. Only the m_H = 170 GeV mass point was studied for the WH channel, where signal events were generated with the MC@NLO program [8].

Table 1 summarizes the most important characteristics of the signal samples used for this note.

Table 1: Signal samples generated for the $t\bar{t}H$ and $WH, H \to WW^{(*)}$ analyses.

Process	m_H [GeV]	σ_{tot}(NLO) [fb]	Final states	Generator	$\sigma \times BR \times \varepsilon_{filter}$ [fb]	N(events)
$t\bar{t}H$	120, 130, 140	669, 534, 431	$t\bar{t}H \to 4W$ (2L)	PYTHIA 6.4	3.60, 6.25, 8.51	∼40k
	150, 160, 170	352, 291, 243			9.68, 10.49,9.31	per m_H
	180, 190, 200	204, 174, 149			7.62, 5.50, 4.42	
$t\bar{t}H$	120, 130, 140	669, 534, 431	$t\bar{t}H \to 4W$ (3L)	PYTHIA 6.4	2.34, 4.05, 5.49	∼40k
	150, 160, 170	352, 291, 243			6.31, 6.91, 6.15	per m_H
	180, 190, 200	204, 174, 149			5.00, 3.54, 2.86	
WH	170	511	$WH \to WWW$ (3L)	MC@NLO	3.42	80k

2.2 Background samples for $t\bar{t}H, H \to WW^{(*)}$

The main backgrounds for the $t\bar{t}H, H \to WW^{(*)}$ final states are $t\bar{t}$, $t\bar{t}W$, $t\bar{t}Z$, $t\bar{t}t\bar{t}$ and $t\bar{t}b\bar{b}$. Single top events have been neglected. Jets from QCD production and WZ production processes are also sources of background. However, lepton identification with isolation and a jet multiplicity requirement are expected to reject a large fraction of these. The background from QCD multijet production has not been properly estimated so far and it is hoped that the selection requirements reduce it to an acceptable level.

A special MC@NLO sample is filtered for a pair of like-sign or more than two leptons with a $p_T > 13$ GeV and $|\eta| < 2.6$ at the generator level. It results in a filter acceptance of 0.0384. In addition, when there are three or more generated leptons, events with oppositely charged leptons from W bosons falling into a special domain ($p_T \geq 30$ GeV and $||\eta| - 1.5| \leq 0.2$ for electron, $p_T \geq 15$ GeV and $||\eta| - 1.25| \leq 0.2$ for muon) were rejected. This results in a small bias, analysis dependent.

The $Wb\bar{b}$ sample was produced by the ALPGEN generator with only leptonic W boson, a generator level filter led to an additional 0.02 acceptance, and a 2.57 K-factor [6] was also included. Leading order $t\bar{t}W + jets$ samples were produced with ALPGEN [9]. The minimum p_T for the additional jets was 15 GeV, while the maximum $|\eta|$ was 6.0. The generated jets were also required to be separated by a distance $\Delta R = \sqrt{\Delta\eta^2 + \Delta\phi^2}$ larger than 0.4. MLM matching [9] was performed to avoid double counting of additional jets.

Samples of $t\bar{t}Z$, $t\bar{t}t\bar{t}$, $t\bar{t}b\bar{b}$ and $t\bar{t}b\bar{b}$(EW) were produced with the leading order generator ACERMC [10]. The $t\bar{t}Z$ events are normalized to the total cross-section recently calculated at NLO [11], while other ACERMC samples are normalized to LO. In the $t\bar{t}Z$ sample, the decay $Z \to \ell\ell$ was forced. The $t\bar{t}b\bar{b}$(EW) sample contains the electroweak contribution to the production of $t\bar{t}b\bar{b}$. For both $t\bar{t}b\bar{b}$ samples, the final states containing four b-jets, two light jets and a lepton (muon or electron) were generated. Table 2 summarizes the characteristics of all background samples relevant for the $t\bar{t}H$ analysis.

2.3 Background samples for $WH, H \to WW^{(*)}$

The $t\bar{t}$ and $Wb\bar{b}$ samples as given in Table 2 are used also in this analysis. For the irreducible diboson WZ/ZZ backgrounds only the fully leptonic decays were considered; this was done with the MC@NLO generator. The ALPGEN $t\bar{t}W$+0 jet sample described in Section 2.2 was analyzed to account for the $t\bar{t}W$ background and as it gives a negligible accepted cross-section the samples with additional jets were not considered. The huge W+jet background was generated with HERWIG [12] and was normalized to the NLO production cross-section [6] with a filter applied, requiring at least one electron (muon) with $p_T \geq 10$ GeV and $|\eta| \leq 2.7$ ($p_T \geq 5$ GeV and $|\eta| \leq 2.8$).

An overview of all background samples used for the WH analysis is given in Table 3.

Table 2: The samples used to estimate the background contribution in the $t\bar{t}H, H \to WW^{(*)}$ analysis. $\mathscr{L}$ denotes the effective integrated luminosity available from Monte Carlo statistics.

Process	Generator	σ_{tot} [fb]	$\sigma \times BR \times \varepsilon_{filter}$ [fb]	N(events)	$\mathscr{L}$ [fb^{-1}]
$t\bar{t}$	MC@NLO	833000	450000	440k	0.98
$t\bar{t}$ pre-filtered	MC@NLO	833000	32000	350k	10.9
$t\bar{t}b\bar{b}$(EW)	ACERMC 3.3	900	244	6.5k	26.6
$t\bar{t}b\bar{b}$	ACERMC 3.3	8200	2244	44k	19.6
$Wb\bar{b}$	ALPGEN	2.1×10^5	1387.8	20k	14.4
$t\bar{t}W$ + 0 jets	ALPGEN	189	25.3	20k	790
$t\bar{t}W$ + 1 jets	ALPGEN	156	20.7	20k	966
$t\bar{t}W$ + $\geq$ 2 jets	ALPGEN	237	34.0	18k	529
$t\bar{t}Z$	ACERMC 3.4	1090	87.0	19k	218
$gg \to t\bar{t}t\bar{t}$	ACERMC 3.4	2.2	1.44	21k	14583
$qq \to t\bar{t}t\bar{t}$	ACERMC 3.4	0.48	0.31	7k	22580

Table 3: List of background samples for the WH analysis. $\mathscr{L}$ denotes the effective integrated luminosity available from Monte Carlo statistics.

Process	Generator	σ_{tot} [fb]	$\sigma \times BR \times \varepsilon_{filter}$ [fb]	N(events)	$\mathscr{L}$ [fb^{-1}]
$t\bar{t}$ no all-hadronic	MC@NLO	833000	450000	440k	0.98
$t\bar{t}$ pre-filtered	MC@NLO	833000	32000	350k	10.9
WZ	MC@NLO 3.10	47760	750	36k	48
ZZ	MC@NLO 3.10	14750	72.5	50k	690
W+jets	HERWIG	1.91×10^8	2.8×10^7	60k	0.0214
$Wb\bar{b}$	ALPGEN	2.1×10^5	1387.8	20k	14.4
$t\bar{t}W$ + 0 jet	ALPGEN	189	25.3	20k	790

3 Selection of the $t\bar{t}H$, $H \to WW^{(*)}$ two and three-lepton final states

In this study, the high p_T single lepton trigger is used for the $t\bar{t}H$ two-lepton ($2L$) events and three-lepton ($3L$) analyses, with a trigger efficiency larger than 96% for both channels at offline selection level. Cut-based analyses were performed, based on the standard ATLAS reconstruction of a medium quality electron [13], combined muons [14], and cone size of $\Delta R = \sqrt{\Delta\eta^2 + \Delta\phi^2} = 0.4$ (cone-0.4) tower jets [15].

Signal data sets for nine Higgs boson masses in the range between 120 and 200 GeV were analysed. In the following, numbers will be given mainly for the most promising Higgs boson mass of 160 GeV including cut flow information for the 120 and 200 GeV mass points.

3.1 Event selection in $t\bar{t}H$, $H \to WW^{(*)}$

The event selection is based on the analysis of final states with at least two reconstructed leptons and jets; from now on we refer to this analysis as "basic selection". Each lepton or jet is required to have transverse momentum $p_T > 15$ GeV and to lie in the pseudorapidity region $|\eta| < 2.5$. Finally, two-lepton ($2L$) events are required to have at least six reconstructed jets, while events with three leptons ($3L$) must have at least four jets.

The $2L$($3L$) selection retains 36.1% (35%) of the Higgs boson events with $m_H = 160$ GeV, while reducing the various backgrounds (see Tables 4 and 5).

For both selections, further suppression of the main background sources can be done by isolation. The isolation criteria require that the transverse energy deposited in the calorimeter around the lepton in a cone size $\Delta R = 0.2$ be below 10 GeV (calorimeter isolation), the maximum p_T of extra tracks reconstructed in the Inner Detector around the lepton track in a cone size $\Delta R = 0.2$ be below 2 GeV

(tracker isolation) and the angular separation $\Delta R_{lep-clj}$ between the lepton and the closest jet be greater than 0.2 for an electron or 0.25 for a muon (cone isolation). This is referred to as "standard isolation" and it allows the reduction of the $t\bar{t}$ background by more than a factor of 10 (170) in the $2L$ ($3L$) analysis. The $t\bar{t}Z/t\bar{t}W$ backgrounds are suppressed by a factor 2 ($t\bar{t}Z$, $2L$) to 5 ($t\bar{t}W + 2$jets, $3L$).

Further reduction of the $t\bar{t}$ background in the dilepton final state can be achieved by requiring exactly two like-sign isolated leptons. This requirement suppresses the large $t\bar{t}$ processes with two leptonic W-decays, as well as the contribution from the $t\bar{t}Z$ process.

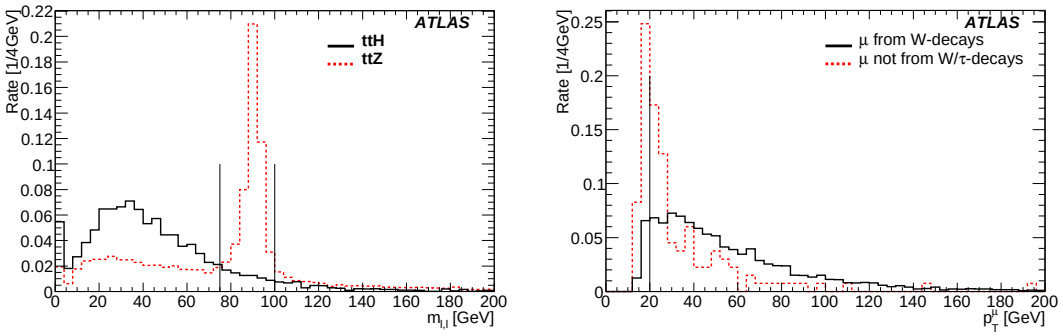

(a) Dilepton invariant mass distributions (b) p_T-distributions of isolated and non-isolated muons

Figure 1: (a) Dilepton invariant mass distributions in $t\bar{t}H$ ($2L$) and $t\bar{t}Z$ and (b) p_T-distributions of muons passing the loose isolation criteria. The solid distribution shows electrons from W decays in the 160 GeV signal sample, the dotted distribution shows muons in $t\bar{t}$, which could not be matched to a generator-level muon from a W- or τ-decay. All distributions are normalized to unity.

In both final states, $t\bar{t}Z$ can be suppressed further by an explicit Z-veto: events that contain a lepton pair of opposite charge and same flavour with an invariant mass between 75 GeV $< m_{\ell\ell} <$ 100 GeV are rejected. This veto includes all leptons passing the selection criteria and loose p_T-cut, here set to 6 GeV. The dilepton invariant mass distributions in $t\bar{t}H$ and $t\bar{t}Z$ are shown in Figure 1(a). The Z-veto decreases the $t\bar{t}Z$-contribution roughly by 75%, while 98% of the signal survive in the $2L$ analysis. In the $3L$ case, 83% of the signal events pass the Z-veto, while 80% of the $t\bar{t}Z$ contribution is suppressed.

At this stage of the $2L$ selection, 73% of the remaining $t\bar{t}$ events have at least one muon from a semi-leptonic heavy quark decay, while the fraction of events with electrons of this origin is only 20% (identification of electrons embedded in jets is more difficult than that of muons).

Further rejection of these muons from $t\bar{t}$ events is achieved by requiring the reconstructed muon p_T to be larger than 20 GeV, as leptons from heavy quark decays tend to be softer than leptons from W decays (see Figure 1(b)). After this cut, the fraction of events with at least one muon from semileptonic decay versus the one with at least one electron from semileptonic decay is respectively 46% and 41% .

The detailed cut flows, with the corresponding accepted cross-sections, are listed in Tables 4 and 5. From now on the "basic selection" is quoted with the filter efficiency allowed for. In the $2L$ analysis we have used the special MC@NLO$t\bar{t}$ sample described in Section 2.2 and a small bias has been computed at various stages of the cut flow. The different values have been found to be compatible and a correction of 1.15 ± 0.10 has been applied in the $t\bar{t}$ line in Table 4. In the $3L$ analysis the standard MC@NLO$t\bar{t}$ sample has been used, and therefore no correction has been applied.

In both cases, the largest background contribution is expected from $t\bar{t}$ events. The accuracy of the MC prediction of the total background expectation is limited by the available statistics and by the intrinsic accuracy of the simulation tools. In the case of $t\bar{t}$ the basic cross-section error is large, but the ALPGEN predictions for higher additional jet multiplicities suffer from even larger uncertainties. There may also

be background contributions from W bosons with multijets which have not been reliably estimated or QCD multijet production or other sources which it has not been possible to simulate.

Table 4: Cut flow and expected cross-sections [fb] for the $t\bar{t}H$ ($2L$) analysis. The errors presented are statistical only. Some backgrounds, such as W+jets, $b\bar{b}$ and $t\bar{t}jj$ have not been included.

Sample	$\sigma_{Total} \cdot BR$	Basic sel.	Calo iso.	Track iso.	Cone iso.	Like-sign	Z-veto	$p_T{}^{\mu}$
$t\bar{t}H$ ($2L^{truth}$, 120 GeV)	3.9	1.05	0.80	0.65	0.52	0.52	0.51	0.45±0.01
$t\bar{t}H$ ($2L^{truth}$, 160 GeV)	11.1	4.01	3.02	2.57	2.09	2.09	2.04	1.85±0.03
$t\bar{t}H$ ($2L^{truth}$, 200 GeV)	4.7	1.83	1.43	1.24	1.05	1.04	1.02	0.95±0.01
$tt\bar{b}\bar{b}$ (EW)	259.0	15.8	4.1	0.9	0.3	0.2	0.2	0.11±0.07
$t\bar{t}b\bar{b}$	2360.	177.	31.7	6.3	1.8	0.9	0.9	0.5±0.2
$t\bar{t}$	833000.	6170.	1970.	870.	500.	16.0	16.0	7.4±1.1
$t\bar{t}t\bar{t}$	2.68	0.65	0.33	0.26	0.20	0.07	0.07	0.06±0.00
$t\bar{t}W$+0j	61.1	1.17	0.46	0.30	0.19	0.10	0.10	0.09±0.01
$t\bar{t}W$+1j	50.5	2.09	0.93	0.66	0.48	0.23	0.23	0.21±0.02
$t\bar{t}W$+≥2j	76.9	8.6	4.9	4.1	3.3	1.58	1.54	1.40±0.05
$t\bar{t}Z$	110.	25.7	20.5	18.1	13.7	1.6	1.2	1.14±0.07
$Wb\bar{b}$	66721.	1.6	0.14	-	-	-	-	-
Total background								10.3±1.1

Table 5: Cut flow and expected cross-sections [fb] for the $t\bar{t}H$ ($3L$) analysis. The errors presented are statistical only; systematic uncertainties are also important. Some backgrounds, such as W+jets, $b\bar{b}$ and $t\bar{t}jj$ have not been included.

Sample	$\sigma_{Total} \cdot BR$	Basic sel.	Calo iso.	Track iso.	Cone iso.	Z-veto	$p_T{}^{\mu}$
$t\bar{t}H$ ($3L^{truth}$, 120 GeV)	2.5	0.66	0.46	0.38	0.29	0.24	0.20±0.00
$t\bar{t}H$ ($3L^{truth}$, 160 GeV)	7.1	2.53	1.78	1.47	1.14	0.95	0.82±0.02
$t\bar{t}H$ ($3L^{truth}$, 200 GeV)	3.1	1.16	0.82	0.70	0.55	0.43	0.39±0.01
$t\bar{t}$	833000.	1600.	230.	50.0	9.3	7.2	2.1±2.1
$t\bar{t}W$+0j	61.1	0.78	0.17	0.08	0.04	0.03	0.03±0.01
$t\bar{t}W$+1j	50.5	1.07	0.28	0.14	0.08	0.08	0.06±0.01
$t\bar{t}W$+≥2j	76.9	2.77	0.85	0.60	0.50	0.42	0.38±0.03
$t\bar{t}Z$	110.	15.0	8.6	6.8	5.3	1.05	0.86±0.06
Total background							3.4±2.1

3.2 Projective likelihood estimator for electron isolation

A projective likelihood estimator, called IsolationLikelihood [13], was developed in the course of the $t\bar{t}H, H \to WW^{(*)}$ ($2L$) analysis. Alternative to the standard isolation, this tool is meant to combine the separation power of several isolation variables into a single, more powerful one. It uses the likelihood ratio method to reject electrons from semi-leptonic heavy quark decays using a different set of isolation variables than those described in Ref. [13]:

- The additional transverse energy deposited in a cone of size $\Delta R = 0.2$ around the electron cluster.
- The sum of the p_{T}^2 of all additional tracks measured in a $\Delta R = 0.2$ cone around the electron cluster.
- The transverse impact parameter significance $|Ip|/\delta(Ip)$ of the electron.

In addition, the "cone isolation" cut is also used as in the standard isolation analysis.

When tuned to give the same electron isolation efficiency obtained with standard isolation in the $t\bar{t}H$ analysis, the IsolationLikelihood allows a higher rejection of non isolated electron background by a factor 1.5 to 4, as shown in Figure 2. Using this projective likelihood estimator could suppress the $t\bar{t}$ background from 7.4 ± 1.1 pb to 5.7 ± 1.0 pb, while keep the same signal and other backgrounds

selection efficiencies. It shows a potential improvement of this analysis which could be adopted at a small increase in complexity, but it has not been used in this document.

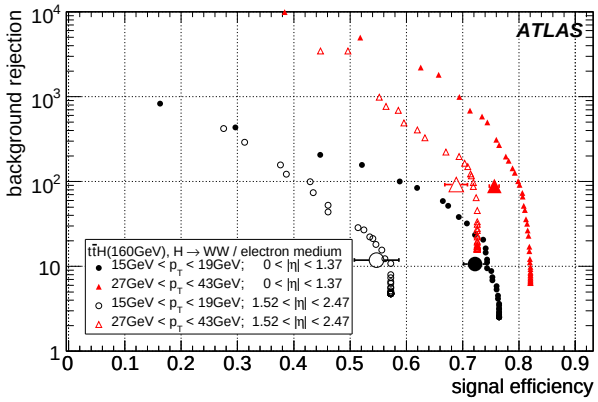

Figure 2: Non-isolated electron rejections vs. signal efficiencies obtained by the IsolationLikelihood estimator for four different p_T and η intervals. The large points mark the working point of the standard isolation cuts for comparison and indicate the size of the error bars, which are not shown for the curves.

4 WH analysis

Only the three lepton final state, $W(H \rightarrow WW^{(*)}) \rightarrow 3\,(l\nu)$ is described below. The analysis of the larger cross-section dilepton final state, which has an important $W + jet$ background is currently ongoing.

The basic selection requires three leptons that satisfy the lepton identification criteria, i.e. medium electron [13] and standard muon [14]. The lepton p_T-thresholds were set to 35 GeV for the leading and 15 GeV for the other lepton. As seen from Fig. 3(a) the cut on the leading lepton reduces the backgrounds much more than the signal. The presence of these leptons also ensures that any signal is efficiently recorded by the ATLAS trigger system

In addition to a 6 GeV calorimeter isolation and a 0.25 cone isolation as described in Section 3.1, $p_{\mathrm{T}}^{track}/p_{\mathrm{T}}^{lepton} \leq 0.05$ were forced, where p_{T}^{track} is of the track with maximal p_T in a cone of ΔR=0.2 (0.3) around the muon (electron). Furthermore, a cut on the lepton three-dimensional impact parameter $I_{3D}/\sigma_I \leq 2.5$ was employed to reject leptons from bottom quarks.

In order to reduce the WZ background, a Z veto is applied by requiring that no opposite sign and same flavor lepton pair has an invariant mass between mass 65 and 105 GeV (Fig. 3(b)). In addition only events with $E_{\mathrm{T}}^{\mathrm{miss}} \geq 30$ GeV were kept. To further reduce the backgrounds, we ask the sum of the p_T of all the jets (which were preselected above 20 GeV from cone-0.7 tower jets [15]) to be smaller than 120 GeV, as seen in Figure 3(c).

For additional rejection of $t\bar{t}$ and $t\bar{t}W$, events having at least one jet fulfilling a loose b-tag [16] are removed. In order to exploit the spin correlations in the $H \rightarrow WW^{(*)}$ signal, the minimum angular separation (ΔR) between lepton pairs is required to be in the range of [$0.1 \sim 1.5$] (so called "H-S cut").

Table 6 summarises the cross-sections after the cut flow described above. The filtered MC@NLO$t\bar{t}$ sample described in Section. 2.2 has been used here. In order to take into account the bias introduced by this sample, a correction of 2.36 ± 0.6 has been applied. The background rate from W bosons with multijets, QCD multijet production or other sources, which have not yet been possible to simulate, have their contribution still under study. The errors on the background are, at this stage, much larger than the size of the expected signal.

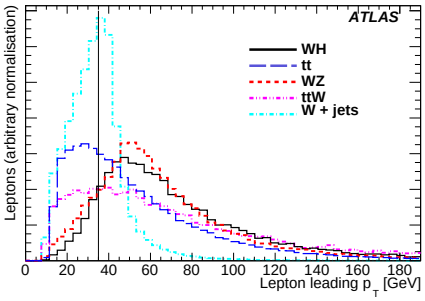

(a) Lepton p_T

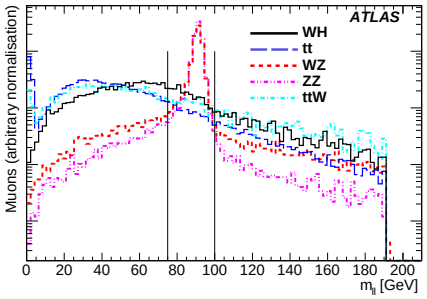

(b) lepton-lepton invariant mass

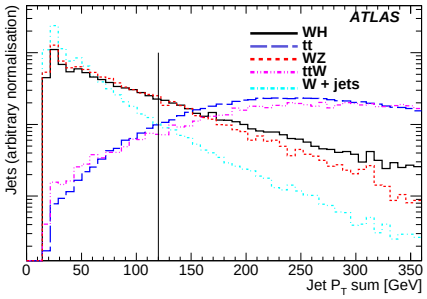

(c) Jet p_T-sum

Figure 3: p_T-distribution for the leading leptons in the $WH(3L)$ signal, $t\bar{t}$, WZ, $t\bar{t}W$ and W+jet-production(a), invariant mass of all the lepton pairs (b) and sum of the p_T of all jets (c) for the WH (3L) signal and the relevant backgrounds. All these plots are done after loose cut.

5 Discussion

5.1 Uncertainties in the analyses

Several systematic uncertainties affect the results presented in this paper. There are theory uncertainties associated to the the choice of the Parton Distribution Functions (PDFs), to the choice of the renormalization and factorization scales, to the description of the initial and final state radiation and to the model used to simulate the heavy quark fragmentation. In order to evaluate the size of these uncertainties, the theory parameters above mentioned have been varied within intervals corresponding to sensible choices. Concerning the PDFs, the MRST2000-LO set was used at the place of the CTEQ6L1.

For the $t\bar{t}H$ analysis, the theory uncertainties have been found to induce a 9% change of the signal cross-section, dominated by the PDF choice. The impact to the $t\bar{t}$ process, which is the most important source of background to this signal, has been found to be 12% in Ref. [6]. An additional 5%, found in study of the signal process, associated to the uncertainty of the initial and final state radiation, has been included in quadrature, giving an overall 13% uncertainty on the total cross-section. However, the background sample is dominated by $t\bar{t}$ with extra jets, and the uncertainty on this rate is of order a factor two. For WH, the PDF uncertainty was found to be less than 5%, and energy scale uncertainty even smaller [17]. Including these effects and others (ISR,FSR) we get a total theoretical uncertainty of 9%.

The effect of experimental systematic uncertainties has been also investigated. The main sources of these uncertainties are represented by the knowledge of the integrated luminosity, the energy scale and the energy resolution of electrons, muons and jets, as well as the tag efficiency of b-jets and the rejection of light quarks. The level of these uncertainties and the impact on the overall event selection is presented

Table 6: WH (3L) cut flow and corresponding cross-sections. The errors presented are statistical only; systematic uncertainties are also important. Some backgrounds, such as WWW, single top and $t\bar{t}Z$ have not been included.

	Input [fb]	Basic sel.	Isolation	Z-veto	$E_{\mathrm{T}}^{\mathrm{miss}}$	H-S	(b-) jet veto
WH (3L)	5.04	1.18	0.62	0.53	0.47	0.36	0.31 ± 0.02
WZ	750.	165.5	1.41	0.74	0.63	0.21	$0.10^{+0.08}_{-0.06}$
$t\bar{t}$	833000.	3564.3	6.45	6.11	5.10	1.02	$0.34^{+0.70}_{-0.3}$
ZZ	72.5	34.5	0.13	0.06	0.013	0.008	0.005 ± 0.001
$t\bar{t}W$	61.1	1.35	0.22	0.21	0.19	0.07	$0.003^{+0.005}_{-0.003}$
$Wb\bar{b}$	66721.	3.1	-	-	-	-	-
$W \to e\nu$+jets	$2.05 \cdot 10^7$	17.6	-	-	-	-	-
$W \to \mu\nu$+jets	$2.05 \cdot 10^7$	27.6	-	-	-	-	-
Total background							0.45 ± 0.70

in Tables 7 and 8. Pile-up events will decrease the detector performance and the impact needs to be properly addressed in future studies. However, the relatively low jet transverse momentum threshold of 15 GeV in the $t\bar{t}H$ analyses may be sensitive to this. The overall systematic uncertainty expected in the $t\bar{t}H$ analysis is 10% (10%) for the 2L (3L) signal and 15% (18%) for those backgrounds which have been quantified. In the case of the WH analysis the overall systematic uncertainty is about 10% for the signal, and about 20% for those background systematics which have been estimated. In each case the total background uncertainty is much larger than this at present.

Table 7: Overview of the experimental systematic uncertainties on the signal and background predictions related to the $t\bar{t}H$ channel in those channels studied. All numbers are in %.

Source of the uncertainty		$t\bar{t}H$ (2L)		$t\bar{t}H$ (3L)	
		Δ signal (%)	Δ background (%)	Δ signal (%)	Δ background (%)
Luminosity	3	3	3	3	3
Electron ID efficiency	0.2	0.2	0.2	0.3	0.3
Muon ID efficiency	1	1.0	1.0	1.5	1.5
Electron E_{T} scale	0.5	0.1	0.1	0.2	0.3
Muon E_{T} scale	1	0.5	0.2	0.7	1.0
Electron E_{T} resolution		0.1	0.1	0.1	0.2
Muon p_T resolution		0.6	2.2	0.3	0.9
Jet energy scale	7	1.2	4.9	2.7	10
Jet energy resolution		1.0	1.4	1.9	5.7
Electron isolation efficiency	1	1	1	1.5	1.5
Muon isolation efficiency	1	1	1	1.5	1.5
Experimental uncertainty		± 3.9	± 6.6	± 5.2	± 12.3

5.2 Conclusion

The $t\bar{t}H, H \to WW^{(*)}$ and $WH, H \to WW^{(*)}$ processes have been studied using two- and three-lepton final states. The signal and main backgrounds have been estimated using a full GEANT based simulation of the detector. The estimated accepted cross-sections in fb of signal and background for these processes are 1.9:10 ($t\bar{t}H$ 2L), 0.8:3.4 ($t\bar{t}H$ 3L) and 0.3:0.4 (WH 3L) respectively. The signal is small and clear distinguishing features such as resonance peaks have not been established. The backgrounds are larger and their uncertainties have not been fully controlled. The analysis is therefore very challenging.

Accurate estimations of the background level using large simulation samples (made with more efficient simulation packages) as well as direct measurements using control samples from real LHC data are essential if a good signal significance is to be reached. For example the production of W bosons with

Table 8: Overview of the experimental uncertainties on the signal and background predictions related to the WH channels in those channels studied. All numbers are in %.

Source of the uncertainty		WH 3L selection				
		$\Delta\, WH$ (3L) (%)	$\Delta\, WZ$ (%)	$\Delta\, t\bar{t}$ (%)	$\Delta\, ZZ$ (%)	$\Delta\, t\bar{t}W$ (%)
Luminosity	3	3	3	3	3	3
Electron ID efficiency	0.2	0.3	0.3	0.2	0.9	1.1
Muon ID efficiency	1	1.5	1.7	1.9	1.0	1.7
Electron energy scale	0.5	0.06	0.06	0.2	0.02	0.07
Muon energy scale	1	0.2	0.1	1.0	0.08	0.7
Muon p_T resolution		0.1	0.03	0.2	0.02	0.4
Jet energy scale	7	2.5	2.6	17.4	2.3	13.6
Jet energy resolution		0.005	0.03	1.9	0.5	0.7
b-tag eff. / light jet rej.	5 / 32	1.0	1.0	2.7	0.8	3.2
Experimental uncertainty		$\pm$4.3	$\pm$14.5			

large numbers of jets need to be measured, as does the fake contribution from b-jets. These two channels should then contribute to the measurement of the Standard Model Higgs boson properties, in particular the couplings of this boson to top and to the W.

References

[1] ATLAS Collaboration, Introduction on Higgs Boson Searches at the Large Hadron Collider, this volume.

[2] ATLAS Collaboration, Higgs Boson Searches in Gluon Fusion and Vector Boson Fusion using the $H \to WW$ Decay Mode, this volume.

[3] J. Levêque, J. B. de Vivie, V. Kostioukhine and A. Rozanov, Search for the standard model Higgs Boson in the $t\bar{t}H$, $H \to WW^{(*)}$ channel, ATL-PHYS-2002-019 (2002).

[4] K. Jakobs, A study of the associated production WH with, $W \to l\nu$ and $H \to WW^{(*)} \to l\nu l\nu$, ATL-PHYS-2000-008 (2000).

[5] V. Cavasinni and D. Costanzo, Search for WH $\to$ WWW $\to l^{\pm}\nu\, l^{\pm}\nu$ jet-jet, using like-sign leptons., ATL-PHYS-2000-013 (2000).

[6] ATLAS Collaboration, Cross-Sections, Monte Carlo Simulations and Systematic Uncertainties, this volume.

[7] T. Sjostrand, S. Mrenna and P. Skands, JHEP **05** (2006) 026.

[8] S. Frixione B. R. and Webber, The MC@NLO 3.2 event generator, 2006, hep-ph/0601192.

[9] M. L. Mangano, M. Moretti, F. Piccinini, R. Pittau and A. D. Polosa, JHEP **07** (2003) 001.

[10] B. P. Kersevan and E. Richter-Was, The Monte Carlo event generator AcerMC version 2.0 with interfaces to PYTHIA 6.2 and HERWIG 6.5, 2004, hep-ph/0405247.

[11] Lazopoulos, Achilleas and McElmurry, Thomas and Melnikov, Kirill and Petriello, Frank, (arXiv:0804.2220[hep-ph]).

[12] G. Corcella et al., HERWIG 6.5 release note, 2002, hep-ph/0210213.

[13] ATLAS Collaboration, Reconstruction and Identification of Electrons, this volume.

[14] ATLAS Collaboration, Muon Reconstruction and Identification: Studies with Simulated Monte Carlo Samples, this volume.

[15] ATLAS Collaboration, Jet Reconstruction Performance, this volume.

[16] ATLAS Collaboration, *b*-Tagging Performance, this volume.

[17] O.Brein, A.Djouadi and R.Harlander, Phys.Lett **B579** (2004) 149–156.